Available online at www.sciencedirect.com
SCIENCE DIRECT
Journal of Catalysis 234 (2005) 292–299
JOURNAL OF CATALYSIS
www.elsevier.com/locate/jcat

The role of ferric ion in the photochemical and photocatalytic oxidation of resorcinol

Sai Wei Lam [a], Ken Chiang [a], Tuti Mariana Lim [b], Rose Amal [a,*], Gary K.-C. Low [c]

[a] *ARC Centre for Functional Nanomaterials, School of Chemical Engineering and Industrial Chemistry, The University of New South Wales (UNSW), Sydney, NSW 2052, Australia*
[b] *Institute of Environmental Science and Engineering (IESE), Nanyang Technological University (NTU), Block 2, Unit 237, 18 Nanyang Drive, Singapore 637723*
[c] *Environmental Forensic and Analytical Science Section, Department of Environment and Conservation (NSW), PO Box 29, Lidcombe, NSW 1825, Australia*

Received 23 March 2005; revised 9 June 2005; accepted 16 June 2005

Available online 9 August 2005

Abstract

The oxidation of resorcinol was investigated in homogeneous solutions of ferric nitrate (photochemical) and in heterogenous suspensions of titanium dioxide (photocatalysis). At pH $\leqslant 2$, synergetic effects were observed for both the photochemical and photocatalytic oxidation of resorcinol with varying ferric ion concentrations up to 5 mM. At pH $\geqslant 2.8$, the presence of ferric ion enhanced the photochemical and photocatalytic oxidations of resorcinol at low ferric ion concentrations ($\leqslant$1 mM). Above 1 mM Fe^{3+}, both the photochemical and photocatalytic oxidations of resorcinol were retarded. Spectrophotometric analysis and theoretical calculations showed that both pH and ferric ion concentration controlled the hydrolysis and polymerisation processes, and thus the Fe(III) speciation, for which the hydrolytic speciation of Fe(III) hydroxo-complexes is of vital influence on the oxidation of resorcinol. The enhancement observed in the presence of ferric ion was attributed to the generation of hydroxyl radicals by soluble Fe(III) hydroxo-complexes and their role as charge trapping species. On the other hand, the negative effect observed was due to the formation of Fe(III) as polynuclear complexes and the precipitation of amorphous hydroxide colloids that subsequently led to a decrease in the total concentration of photoactive iron species in solution.

Keywords: Photocatalytic; Photochemical; Titanium dioxide; Resorcinol; Ferric ion

1. Introduction

The public concerns on resorcinol are related to its widespread occurrence in the environment. This compound has been listed as one of the potent endocrine disrupting chemicals [1]. It has been found to interfere with triiodothyronine (T3) and thyroxine (T4) metabolism and interrupt the normal functioning of thyroid system. Hence, this points to the necessity to develop efficient and cost effective methods that would destroy this refractory compound.

To date, advanced oxidation processes (AOPs) appear to be promising methods that provide almost complete oxidation of organics to innocuous products such as carbon dioxide, water and mineral acids under ambient conditions [2–4]. AOPs can be divided into photochemical oxidations (H_2O_2/UV, O_3/UV, Fe^{3+}/UV), semiconductor photocatalysis (TiO_2/UV) and chemical oxidations (O_3, O_3/H_2O_2, H_2O_2/Fe^{2+}). These processes make use of different reactive chemicals and/or catalysts. Nonetheless, they are characterised by a common feature that generate highly reactive radicals for the remediation process.

Among the AOPs, heterogeneous photocatalysis using TiO_2 and photochemical oxidations by Fe^{3+} have received a widespread attention. These techniques eliminate the use of expensive oxidants such as H_2O_2 and O_3. However, TiO_2 photocatalyst suffers from a drawback of low quantum efficiency. Several approaches have been employed to improve

* Corresponding author. Fax: +61-9385-5966.
E-mail address: r.amal@unsw.edu.au (R. Amal).

0021-9517/$ – see front matter
doi:10.1016/j.jcat.2005.06.014

the performance of TiO_2 photocatalyst, including the incorporation of metal in the lattice or at surface of TiO_2, which could alter the rate of electron–hole recombination and/or extend the light absorption into the visible range.

The use of UV/Fe^{3+} has been of interest, since Fe^{3+} is one of the most ubiquitous metal ions in natural water and wastewater streams. Depending on the nature of the pollutant, the beneficial effect of Fe^{3+} can be summarised via different photoprocesses [5]. If the pollutant is an effective metallic complexant, Fe^{3+} could form a complex with the pollutant that exhibits photoactivity under ultraviolet (UV) and/or visible (vis) illumination. Conversely, if Fe^{3+} does not form complex with the pollutant, it could coordinate with water molecules to form hydroxy complexes that would undergo photolysis, giving rise to Fe(II) species and hydroxyl radicals (·OH). Similarly, in the presence of hydrogen peroxide, Fe^{3+} could initiate and photocatalyse the decomposition of hydrogen peroxide, resulting in the generation of ·OH. Moreover, Fe^{3+} could also act as a charge trapping species that retard the recombination of electron–hole pairs in a photocatalytic reaction. Hence, it is the aim of the present study to investigate and compare the oxidation of resorcinol catalysed by the homogeneous UV/Fe^{3+} and the heterogenous UV/Fe^{3+}/TiO_2 reactions. From these experiments, the effect of charge trapping species of Fe^{3+} on the photocatalytic oxidation of resorcinol in aqueous suspension of Degussa P25 TiO_2 will also be addressed.

2. Experimental

2.1. Chemicals

Degussa P25 TiO_2 (80% anatase, 20% rutile) was used as the photocatalyst. The BET surface area and crystal size of these particles were found to be 48 m^2/g and 20–30 nm, respectively [4]. Resorcinol, perchloric acid ($HClO_4$), ferric nitrate ($Fe(NO_3)_3$), ammonium formate (NH_4COOH), formic acid (HCOOH), methanol and *o*-phenanthroline were of analytical grade and used without further purification. All solutions were prepared using water from a Millipore Milli-Q water purification system.

2.2. Photoactivity studies

The photoactivity studies were performed in a cylindrical annular-type photoreactor. The light source used was a 20 W blacklight blue fluorescent tube with an emission range of 300–400 nm and a maximum emission centered at 360 nm. A volume of 600 ml prepared resorcinol solution with an initial concentration of 20 ppm was circulated through the photoreactor. Purified air was introduced continuously into the system at the rate of 100 ml/min to maintain a constant dissolved oxygen level. The oxidation of resorcinol was carried out for up to 4 h. A range of pH values, from 1.5 to 3.3 were chosen. An online pH meter was used to monitor the pH change. Samples were withdrawn intermittently and filtered through 0.45 μm PTFE filters prior to total organic carbon (TOC, Shimadzu T-V_{CSH}) and high performance liquid chromatography (HPLC, Waters 2695) analyses. A mobile phase consisted of a mixture of methanol and 10 mM NH_4COOH with pH adjusted to 3.0 using HCOOH (10/90, v/v) and a reverse phase C18 Atlantis column (4.6 × 250 mm) were used to perform the separation. By means of a photodiode array detector (PDA, Waters 2996), the concentration of resorcinol was measured at 274 nm.

The photocatalytic activity of TiO_2 (0.1 g/l) was also investigated for pH values ranging from 1.5 to 3.3. A volume of 500 ml TiO_2 suspension was dispersed in an ultrasonic bath for 30 min before being added into the reactor. The suspension was illuminated for 30 min in order to remove any residual organic matter in the system. Subsequently the light was turned off, and 100 ml of the resorcinol stock solution was added and mixed with the TiO_2 suspension to give an initial resorcinol concentration of 20 ppm. The slurry was circulated through the reactor for another 15 min in the dark to attain adsorption equilibrium followed by 4 h of photoreaction.

In order to evaluate the effect of iron on the oxidation of resorcinol, $Fe(NO_3)_3$ was added into the TiO_2 suspension. The concentration of Fe^{3+} was varied from 0.5 to 5.0 mM. $Fe(NO_3)_3$ was selected for the present system based on the fact that NO_3^- was known to play an insignificant role on the photodissociation of Fe(III) species to form ·OH [6]. Moreover, NO_3^- has been reported to adsorb weakly onto the TiO_2 surface [7], thereby preserving the active sites for photocatalytic reaction. Despite that, the irradiation of NO_3^- could result in the formation of ·OH [8]. In response to this, the involvement of NO_3^- as a source of ·OH was checked using an ion chromatography (Waters 515) equipped with an ion exchange Dionex IonPac® AS16 column (4 × 250 mm) and a conductivity detector (Waters 432). It was detected that the concentration of NO_3^- to be unchanged throughout the photoreactions. This pointed to the absence of NO_3^- photolysis in the present system. To monitor the change in total iron concentration in solution, inductive coupled plasma (Varian, Vista AX) was used. The concentration of Fe^{2+} was determined by complexometry with *o*-phenanthroline, using an absorption constant of $\varepsilon_{510} = 1.128 \times 10^4\ l\,mol^{-1}\,cm^{-1}$ at 510 nm.

2.3. Hydrolytic speciation and complexation studies of iron

The hydrolytic speciation of $Fe(NO_3)_3$ were analysed from 200 to 600 nm by means of a UV–vis spectrophotometer (Varian, Cary 1E). The pH chosen was in a range of 1.5 to 3.3 with an initial concentrations of $Fe(NO_3)_3$ varied from 0.5 to 5 mM. In order to detect the formation of Fe^{3+}-resorcinol complex, similar measurements were carried out in the presence of resorcinol. The concentration of resorcinol was fixed at 20 ppm.

2.4. Theoretical calculations on the speciation of iron

Theoretical calculations on the speciation of iron in solution were carried out using WIN32-STABCAL. The speciation calculations were carried out at 25 °C. The Fe^{3+} concentration was varied from 0.5 to 5.0 mM. The equilibrium constants of iron species were obtained from the US National Bureau of Standards (NBS).

3. Results and discussion

3.1. Photolysis and photocatalytic oxidation of resorcinol under various pH conditions

It was found that the oxidation of resorcinol was inefficient in the presence of UV alone for the pH range of 1.5 to 3.3, indicating the absence of direct photolysis. A significant oxidation was only observed after the addition of TiO_2. The rate of photocatalytic oxidation of resorcinol decreased in the following sequence: pH 3.3 ≈ pH 2.8 > pH 2 > pH 1.5. This is thought to be related to a lower ·OH production on the surface of photoexcited TiO_2 at lower pH [2]. In addition, the better adsorption of intermediate products onto the TiO_2 surface at higher pH could also enhance the surface reaction [4].

3.2. Effect of ferric ion on the photochemical and photocatalytic oxidation of resorcinol under various pH conditions

Fig. 1 depicts the effect of Fe^{3+} on the initial photochemical mineralisation rate of resorcinol at various pH conditions. The presence of Fe^{3+} accelerated the photochemical mineralisation of resorcinol extensively. At pH ⩽ 2.0, the initial photochemical mineralisation rate of resorcinol increased with increasing Fe^{3+} concentration. Similarly, at pH > 2.0, an analogous trend was observed, except that beyond 1 mM Fe^{3+}, the initial photochemical mineralisation rate of resorcinol dropped despite a further increase in Fe^{3+} concentration. As it can also be seen from Fig. 1, the initial photochemical mineralisation rate of resorcinol at pH 3.3 was found to be the slowest for all Fe^{3+} concentrations studied.

The presence of Fe^{3+} had also affected the initial photocatalytic mineralisation rate of resorcinol in a similar manner as those observed in the UV/Fe^{3+}. Fig. 2 presents the influence of Fe^{3+} on the initial photocatalytic mineralisation rate of resorcinol in the acidic pH range. At pH ⩽ 2.0, the initial photocatalytic mineralisation rate of resorcinol was found to increase with Fe^{3+} concentration. At pH > 2.0, Fe^{3+} enhanced the initial photocatalytic mineralisation rate of resorcinol, reaching an optimal concentration at 1 mM Fe^{3+}. Beyond the optimum point, the presence of Fe^{3+} retarded the initial photocatalytic mineralisation rate of resorcinol. It was also observed that the initial photocatalytic mineralisation rate of resorcinol at pH 2.8 was slower than that at pH 3.3 in the presence of 5 mM Fe^{3+}.

In order to get an insight into understanding of the effect of Fe^{3+} on the kinetic of resorcinol oxidation, the photochemical and photocatalytic degradation of resorcinol were also followed. For all conditions studied, Fe^{3+} had influenced both the photochemical and photocatalytic degradations profiles of resorcinol in an analogous manner as those observed in the mineralisation of resorcinol, with an exception at pH 3.3. Figs. 3a and b compare the influence of Fe^{3+} on the degradation and mineralisation of resorcinol as a function of illumination time at pH 3.3, respectively, both with and without the addition of TiO_2. The presence of Fe^{3+} had affected the photochemical degradation and mineralisation of resorcinol in a similar manner: 0.5 mM > 1.0 mM > 5.0 mM > 0.0 mM Fe^{3+}. Whilst the photocatalytic mineralisation of resorcinol was slightly enhanced for a Fe^{3+} concentration up to 1.0 mM, the photocatalytic degradation

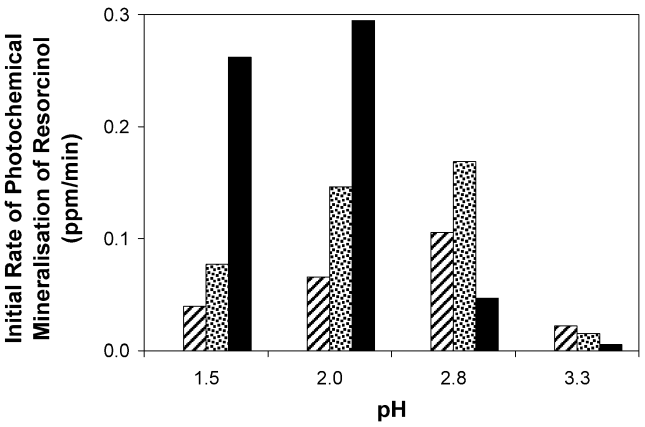

Fig. 1. Effect of ferric ion concentrations: (□) 0 mM, (▨) 0.5 mM, (▩) 1 mM and (■) 5 mM, on the photochemical mineralisation of resorcinol at various pH conditions. Conditions: $[Resorcinol]_0 = 20$ ppm, air flow rate = 100 ml/min.

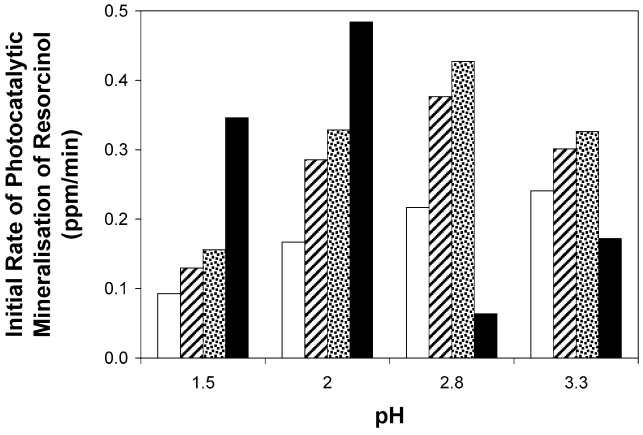

Fig. 2. Effect of ferric ion concentration: (□) 0 mM, (▨) 0.5 mM, (▩) 1 mM and (■) 5 mM, on the photocatalytic mineralisation of resorcinol at various pH conditions. Conditions: $[TiO_2] = 0.1$ g/l, $[Resorcinol]_0 = 20$ ppm, air flow rate = 100 ml/min.

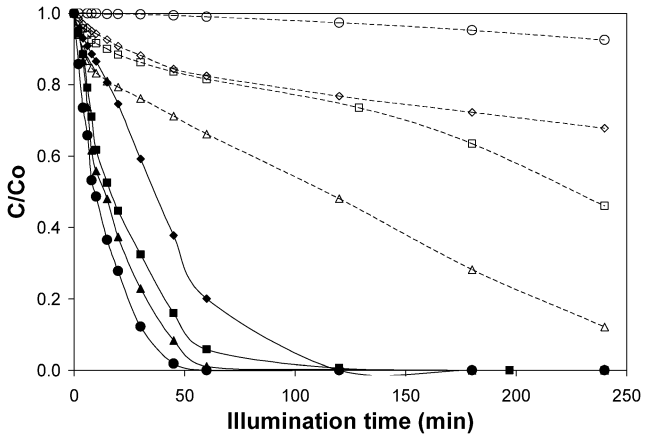

(a)

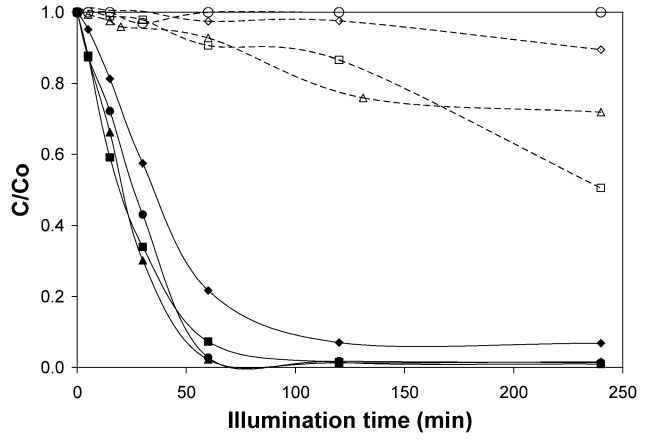

(b)

Fig. 3. Effect of ferric ion concentration on the (a) degradation and (b) mineralisation profile of resorcinol at pH 3.3 under various conditions: UV/Fe^{3+} (○) 0 mM, (△) 0.5 mM, (□) 1 mM and (◇) 5 mM; and UV/Fe^{3+}/TiO_2 (●) 0 mM, (▲) 0.5 mM, (■) 1 mM and (◆) 5 mM. Conditions: $[TiO_2] = 0.1$ g/l, $[\text{Resorcinol}]_0 = 20$ ppm.

of resorcinol was retarded for all the concentrations of Fe^{3+} studied. It was also indicated in Fig. 3 that UV/Fe^{3+} alone was incapable to completely degrade resorcinol.

3.3. The chemistry of ferric ions in solution

In order to elucidate the role of Fe^{3+}, the optical property of the Fe^{3+} solution was analysed spectroscopically. The analysis was carried out in the absence of resorcinol in order to avoid any interference which arises from its absorption in the UV region. Furthermore, theoretical calculations were also performed to model the distribution and speciation of Fe(III) species. Fig. 4 presents the speciation of Fe(III) species as a function of pH.

Many studies have reported that Fe^{3+} hydrolysed in an aqueous solution to form different Fe(III)-hydroxo complexes that are responsible for OH· radicals generation [3,6,9,10]. However, since polymerisation–precipitation reactions proceed at the same time, the monomeric complexes slowly covert to polynuclear complexes and hydroxide colloids [3,6]. In acidic solutions, the major monomeric forms

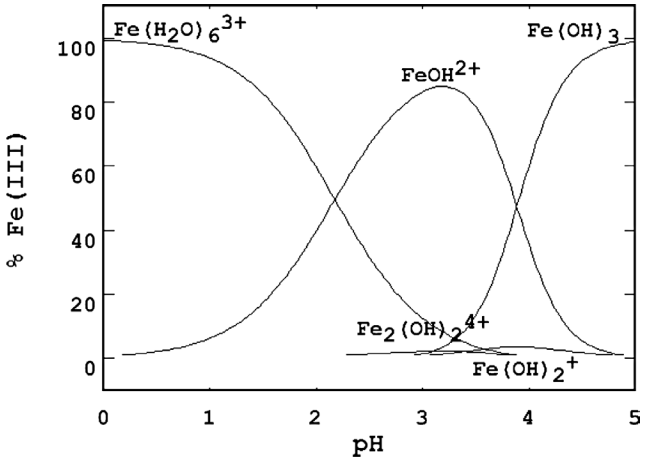

(a)

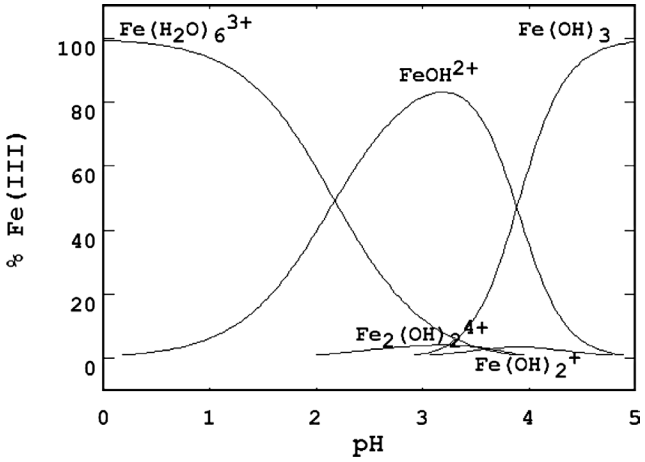

(b)

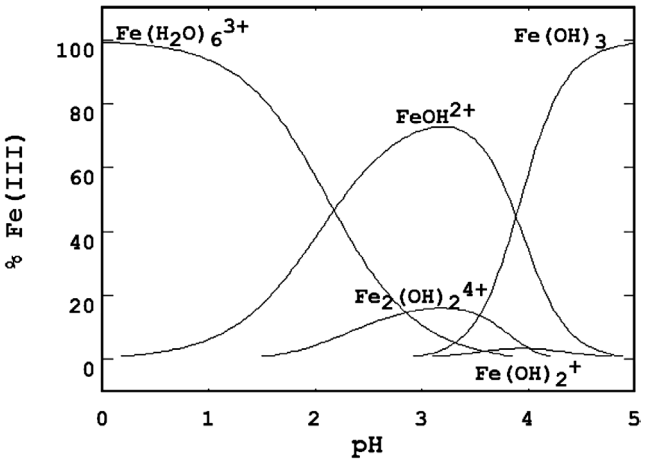

(c)

Fig. 4. Theoretical calculations on the speciation of Fe(III) species using WIN32-STABCAL in the presence of (a) 0.5 mM, (b) 1.0 mM and (c) 5 mM Fe^{3+}.

are $Fe(H_2O)_6^{3+}$, $Fe(OH)^{2+}$ and $Fe(OH)_2^{+}$ [6,9]. These hydroxo complexes feature a unique characteristic of absorption and therefore they can be easily distinguished from their absorption spectra. Fig. 5 shows the absorption spectra of a $Fe(NO_3)_3$ solution in the pH range of 1.5 to 3.3.

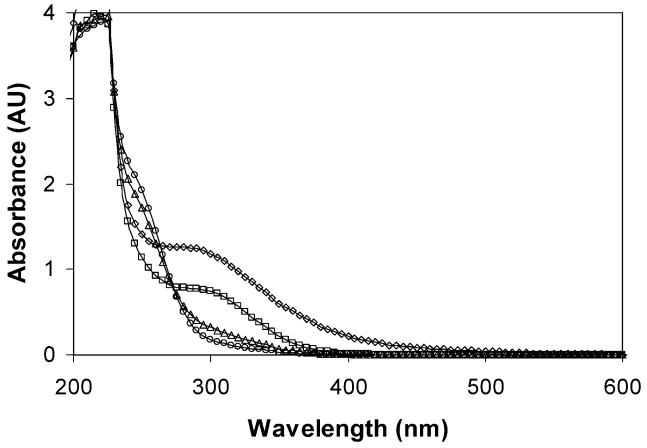

(a)

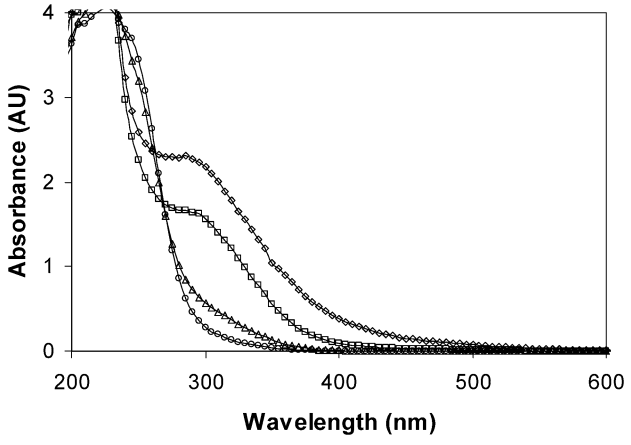

(b)

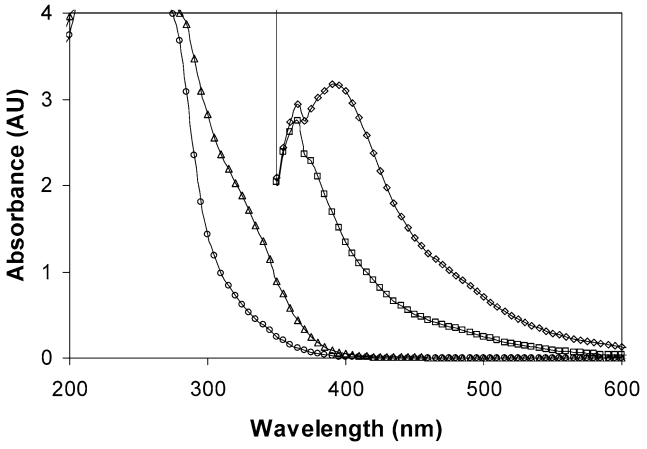

(c)

Fig. 5. UV/vis spectrophotometric analysis of different Fe(III) species in the presence of (a) 0.5 mM Fe^{3+}, (b) 1 mM Fe^{3+} and (c) 5 mM Fe^{3+} at various pH conditions: (○) pH 1.5, (△) pH 2.0, (□) pH 2.8 and (◇) pH 3.3.

As can be seen from Fig. 4, $Fe(H_2O)_6^{3+}$ is the dominant species at pH < 2.5, which agreed to that reported by Langford and Carey [11]. Faust and Hoigne [12] detected that this species exhibited a maximum absorbance at $\lambda = 240$ nm. In comparison, a high absorption at $\lambda = 240$ nm for pH ⩽ 2.0 was also seen in the present study, as shown in Figs. 5a and b. Between pH 1.5 to 4, the predominant species is $Fe(OH)^{2+}$, which was consistent with that observed by Faust and Hoigne [12]. Franck and Klopffer [13] detected the absorption band of this species coincided with UV region (290–400 nm) with a major peak centered at 295 nm. This is again in good agreement with the present observation (see Figs. 5a and b). Another monomeric species, $Fe(OH)_2^{+}$ was found to display an absorption spectra similar to that of $Fe(OH)^{2+}$ [6]. Nonetheless, $Fe(OH)_2^{+}$ exists in low concentration in solution (see Fig. 4). Hence, only a few studies were emphasised on the activity of this species.

The monomeric Fe(III)-hydroxo complexes absorbed strongly in the UV region; this overlapped with the absorbance characteristic of NO_3^- (265–335 nm). As a result, the absorbances reported in Fig. 5 could have been influenced by the presence of NO_3^-. However, it was deduced that, in the present system, NO_3^- contributed only about 1–5% of the total absorbances depending on the concentration of $Fe(NO_3)_3$ in solution. Thus, the absorbances in Fig. 5 are primarily attributed to the Fe(III) species.

The photoactivity of Fe(III)-hydroxo complexes is in general governed by ligand-to-metal charge transfers (LMCT) involving the non-bonding *p*-orbitals in a Fe atom. Among the Fe(III)-hydroxo complexes, $Fe(OH)^{2+}$ has been found to possess the highest quantum yield for the photoproduction of ·OH radicals in acidic solutions [12,14]. On the other hand, the absorption spectrum of $Fe(H_2O)_6^{3+}$ does not significantly overlap the UV region, thereby it contributes insignificantly to the ·OH radicals generation.

Lopes et al. [9] developed the ZINDO/S semiempirical method to model the molecular orbital of Fe(III)-hydroxo complexes. They computed that upon an excitation in the UV region, $Fe(H_2O)_6^{3+}$ and $Fe(OH)^{2+}$ generated excited species of $(Fe^{2+}–H_2O^{+})^*$ and $(Fe^{2+}–{\cdot}OH)^*$, respectively. The generation of $(Fe^{2+}–H_2O^{+})^*$ occurred via an electronic transfer from a non-bonding *p*-orbital centred on a water molecule, while $(Fe^{2+}–{\cdot}OH)^*$ was produced via an electronic transfer from a non-bonding *p*-orbital centred on a hydroxyl ligand. It was also demonstrated in their study that the highest occupied molecular orbital (HOMO) of OH^- ligands had energy higher than that of H_2O, in which it gave rise to $Fe(OH)^{2+}$ photoactivity towards ·OH radicals generation under UV illumination. Furthermore, the removal of ·OH from $(Fe^{2+}–{\cdot}OH)^*$ involved a lower degree of structural transformation compared to $(Fe^{2+}–H_2O)^*$. Hence, this explains the higher quantum yield of $Fe(OH)^{2+}$ photolysis compared to that of $Fe(H_2O)_6^{3+}$.

Besides the pH effect, the hydrolytic speciation of Fe(III)-hydroxo complexes was also markedly influenced by the total iron concentration. Charles and Flynn [15] found that $Fe(NO_3)_3$ in solution was unstable and formed precipitates at pH 2.3 and 3.0 in the presence of 10 and 1 mM Fe^{3+}, respectively. It can been seen from the theoretical calculations in Fig. 4 that the polynuclear complex $(Fe_2(OH)_2^{4+})$ and amorphous hydroxide colloids $(Fe(OH)_3)$ formed favourably at pH > 2 and pH > 3, respectively. Krysova et al. [3] re-

ported a red shift in the absorption of polynuclear complexes and hydroxide colloids into the visible region until 600 nm. A sharp absorption peak was also seen in the present system from 350 to 600 nm, as shown in Fig. 5c, when the concentration of Fe^{3+} was increased from 1 to 5 mM at pH $\geqslant$ 2.8. Therefore, the present findings confirm the occurrence of polymerisation–precipitation mechanisms and they provide the evidences to further support the formation of $Fe_2(OH)_2{}^{4+}$ and $Fe(OH)_3$ at higher Fe^{3+} concentrations.

Brand et al. [16] reported that the $Fe_2(OH)_2{}^{4+}$ possessed a better absorption of energy from the photons than those major monomeric Fe(III)-hydroxo complexes. In spite of that, the $Fe(OH)_2{}^{4+}$ and $Fe(OH)_3$ have very low quantum yields for the photogeneration of ·OH [6]. Consequently, this contributes to an overall drop in photoactivity in the present system at higher pH, in particular at pH 3.3. It is clear that the efficiency of resorcinol oxidation is associated with the nature of Fe(III) species that present in the solution, and $Fe(OH)^{2+}$ is believed to be the key species in acidic solutions controlling the production of ·OH radicals that are responsible for the oxidation of resorcinol.

3.4. The role of ferric ion

The basic step of Fe(III) catalysed photolysis of water is $Fe^{III} + H_2O + h\nu \rightarrow Fe^{II} + OH\cdot + H^+$. To further enhance the understanding of the role of Fe^{3+} during the photochemical and photocatalytic oxidations of resorcinol, the concentration of Fe^{2+} was monitored spectroscopically. Figs. 6 and 7 depict the initial photogeneration rate of Fe^{2+} obtained during the photochemical and photocatalytic oxidations of resorcinol, respectively.

Comparing Figs. 1 and 6, a good correlation can be seen between the initial photogeneration rate of Fe^{2+} and the initial photochemical oxidation rate of resorcinol. The higher the initial photochemical oxidation rate of resorcinol, the higher is the photogeneration rate of Fe^{2+}. When the concentration of Fe^{3+} is significantly low such that the formation of $Fe(OH)_3$ is inhibited, the rate of photogeneration of Fe^{2+} is found to be depended strongly on the concentration of photoactive Fe(III)-hydroxo complexes, mostly the concentration of $Fe(OH)^{2+}$. It can be seen from Fig. 8 that the relative absorbance of Fe^{3+} extracted at 295 nm, which corresponded to the distribution of $Fe(OH)^{2+}$, agreed very well with the initial rate of photogeneration of Fe^{2+}. This is also consistent with the previous studies by Krysova et al. [3], Brand and Bolte [5], Brand et al. [16], Mrowetz and Selli [17] and Mazellier and Bolte [18], where the involvement of $Fe(OH)^{2+}$ in the generation of ·OH for pH range of 2.8 to 3.3 at low Fe^{3+} concentrations (<0.3 mM) was also reported. Fig. 8 also indicated that $Fe(OH)^{2+}$ continued to be the most influential species for the photoproduction of ·OH in the present system at pH $\leqslant$ 2, particularly at high Fe^{3+} concentrations. Emett and Khoe [19] studied the photochemical oxidation of arsenic and found that $Fe(OH)^{2+}$ was an effective source of ·OH at pH 1.5.

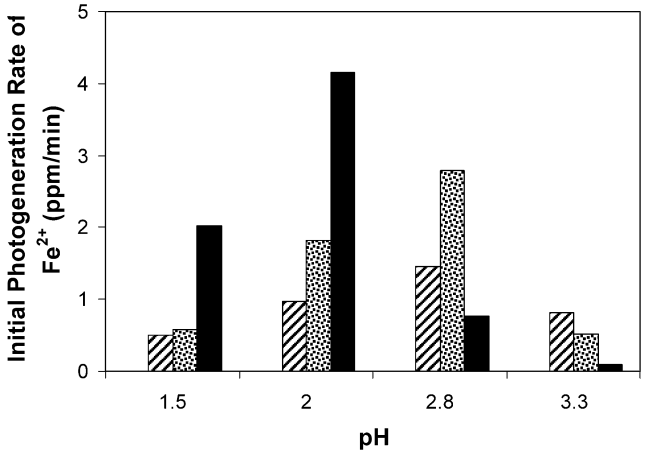

Fig. 6. Effect of pH and ferric ion concentration (▨) 0.5 mM, (▩) 1 mM and (■) 5 mM on the photogeneration of ferrous ion during the photochemical mineralisation of resorcinol. Conditions: $[Resorcinol]_0 = 20$ ppm, air flow rate = 100 ml/min.

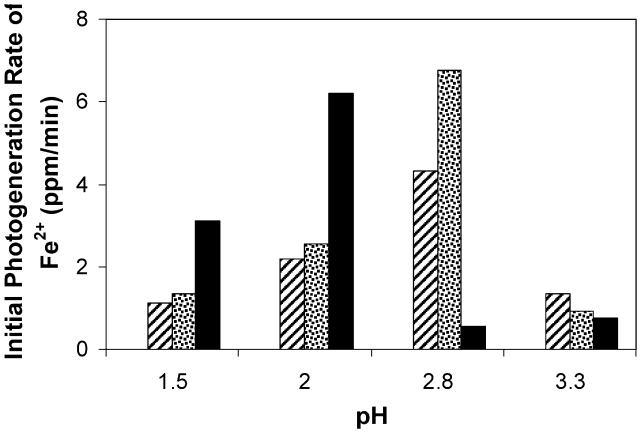

Fig. 7. Effect of pH and ferric ion concentration (▨) 0.5 mM, (▩) 1 mM and (■) 5 mM on the photogeneration of ferrous ion during the photocatalytic mineralisation of resorcinol. Conditions: $[TiO_2] = 0.1$ g/l, $[Resorcinol]_0 = 20$ ppm, air flow rate = 100 ml/min.

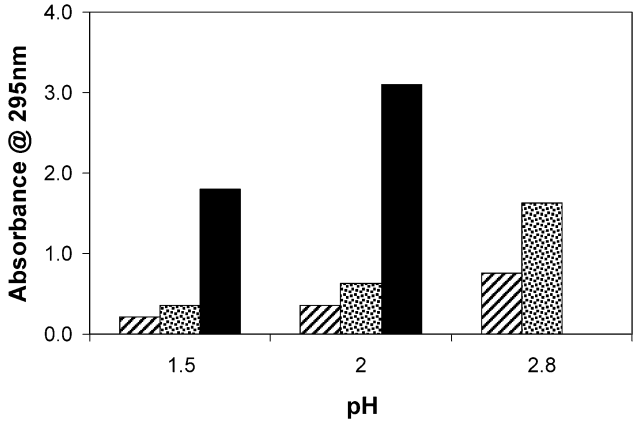

Fig. 8. UV absorbance of Fe(III) species extracted at 295 nm under various pH conditions and ferric ion concentrations, (▨) 0.5 mM, (▩) 1 mM and (■) 5 mM.

On the contrary, the formation of $Fe(OH)_2{}^{4+}$ and $Fe(OH)_3$ at higher pH reduced the concentration of photoactive species in the solution and caused a simultaneous decrease in the photogeneration rate of Fe^{2+} as shown in Fig. 6. Apart from its role as a sink for $Fe(OH)^{2+}$, the $Fe(OH)_3$ may also scatter the light and thus decrease the amount of photon available for catalyst activation. For this reason, the quantification of $Fe(OH)^{2+}$ by absorbance measurement at higher pH becomes inconclusive. Consequently, the absorbance of $Fe(OH)^{2+}$ at pH 2.8 in the presence of 5 mM Fe^{3+} and at pH 3.3 was excluded from Fig. 8.

Comparing Figs. 2 and 7, a discrepancy was observed between the initial photogeneration rate of Fe^{2+} and the initial photocatalytic oxidation rate of resorcinol, particularly at pH 2.8 in the presence of 5 mM Fe^{3+} and at pH 3.3. This observation pointed out that the removal efficiency of resorcinol and its intermediate products from solution in the presence of TiO_2 is not ruled only by the mechanism of photolysis of Fe^{III}/Fe^{II} couple. It has been observed that the pH of solution increased rapidly during the photocatalytic oxidation of resorcinol at pH 2.8 in the presence of 5 mM Fe^{3+} and at pH 3.3. Since iron precipitates favourability at pH > 3 to form $Fe(OH)_3$, it is believed that the disappearance of the organic matters could be governed by the adsorption mechanism. The higher disappearance of organic matters at pH 3.3 compared to pH 2.8, in the presence of 5 mM Fe^{3+}, could be attributed to the greater amount of hydroxide surfaces formed at pH 3.3, which subsequently leads to higher removal of organic matters via adsorption. This is proposed in view of the greater increase in pH of solution at pH 3.3 than pH 2.8. While $Fe(OH)_3$ could have acted as an adsorbent, the enhanced formation of $Fe(OH)_3$ also marked a higher degree of light filtering effect during photoreactions, resulting in the retardation effect at pH 3.3.

It is also noted that in the cases where the formation of $Fe(OH)_2{}^{4+}$ and/or $Fe(OH)_3$ is dominant (i.e., at pH 2.8 in the presence of 5 mM Fe^{3+} and at pH 3.3), the initial photogeneration rate of Fe^{2+} was found to be similar for both UV/Fe^{3+} and $UV/TiO_2/Fe^{3+}$, as revealed in Figs. 6 and 7. On the contrary, at low pH, the initial photogeneration rate of Fe^{2+} was higher in the $UV/Fe^{3+}/TiO_2$ than UV/Fe^{3+}. This could be ascribed to the reduction of Fe^{3+} to Fe^{2+} by the photoexcited electron on the TiO_2 surface. The fact that Fe^{3+} has a more positive redox potential (+0.77 V) than the flat band potential of TiO_2 (−0.3 V) makes the scavenging mechanism of photogenerated electron by Fe^{3+} possible. Accordingly, this also suggests that the monomeric Fe(III)-hydroxo complexes could trap electrons more efficiently than the $Fe(OH)_2{}^{4+}$ and/or $Fe(OH)_3$, thus enhancing the charge carriers' separation and retarding the recombination reaction. Mest'ankova et al. [20] studied the degradation of herbicide monuron in the presence of TiO_2 and $Fe(ClO_4)_3$, and also reported that $Fe(OH)^{2+}$ is an efficient electron scavenger.

Fig. 9 presents a typical mineralisation–time plot and the photogeneration of Fe^{2+} during the photoreactions. As depicted in Fig. 9, the evolution of Fe^{2+} and the mineralisation of resorcinol increased rapidly at the beginning of irradiation. At low Fe^{3+} concentration (⩽1 mM), the reduction of Fe^{3+} to Fe^{2+} slowed down as time proceeded and attained an equilibrium Fe^{2+} concentration (Fe^{2+}_{eq}) of a value that roughly corresponded to the initial concentration of Fe^{3+} added ($Fe^{3+}_{initial}$). However, at 5 mM Fe^{3+}, the Fe^{2+}_{eq} concentration was observed to be lower than its Fe^{3+}_{intial}. It was also found that the deviation between Fe^{2+}_{eq} and $Fe^{3+}_{initial}$ became more significant with increasing pH. Furthermore, at pH 3.3, a lower Fe^{2+}_{eq} concentration was also detected and it remained relatively constant ($Fe^{2+}_{eq} \approx 0.4$ to 0.5 mM) regardless of the Fe^{3+}_{intial}. Since Fe^{2+}_{eq} is indirectly related to the total net production of ·OH, especially in UV/Fe^{3+}, this finding further reinforces the inefficiency of $Fe(OH)_2{}^{4+}$ and $Fe(OH)_3$ in the photoproduction of ·OH. It is also detected that the total dissolved iron concentration at pH 2.8 in the presence of 5 mM Fe^{3+} and at pH 3.3 was below its initial concentration. The effect was more prominent in $UV/Fe^{3+}/TiO_2$ than UV/Fe^{3+}. As Fe^{3+} has been found to adsorb very well onto TiO_2 [17], the difference observed between UV/Fe^{3+} and $UV/Fe^{3+}/TiO_2$ could be caused by the adsorption of Fe^{3+} onto TiO_2.

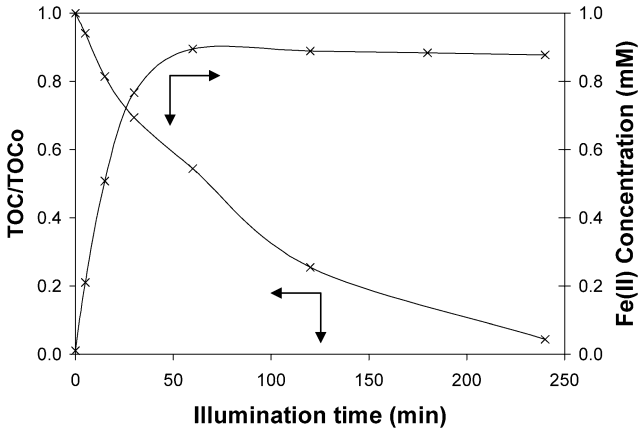

Fig. 9. The relation between mineralisation–time plot of resorcinol and the photogeneration ferrous ions. Conditions: $[Fe^{3+}]_0 = 1$ mM, [Resorcinol]$_0 = 20$ ppm, air flow rate = 100 ml/min, $pH_0 = 2$.

It is also demonstrated in Fig. 9 that the oxidation of resorcinol continued even after Fe^{2+} reached its equilibrium. This reflects the establishment of a dynamic equilibrium, i.e., there is simultaneously photoreduction of Fe(III)-hydroxo complexes into Fe^{2+} and reoxidation of Fe^{2+} by ·OH and/or O_2 to regenerate the photoactive species of Fe(III) for a continuous production of ·OH. However, when Fe^{2+} is reoxidised by ·OH to Fe^{3+}, this may induce a competition for ·OH, which reduces the availability of ·OH for oxidation of organic matters. The involvement of ·OH in the reoxidation of Fe^{2+} was evidenced in the present system. Viewing the fact that the reoxidation of Fe^{2+} to Fe^{3+} is accompanied by the release of OH^- ($Fe^{2+} + {\cdot}OH \rightarrow Fe^{3+} + OH^-$), this corresponded with the increase in pH of solution

detected during the photoreactions at pH 2.8 in the presence of 5 mM Fe^{3+} and at pH 3.3. For all the concentrations of Fe^{3+} added during the photochemical oxidation of resorcinol at pH 3.3, the pH of solution was observed to increase with illumination ($pH_{final} \approx 3.5$–4.3). A very fast increase of the pH of solution up to a constant pH value of 5.1 was also seen during the photocatalytic oxidation of resorcinol at pH 3.3. For longer irradiation times, the pH of solution decreased slowly and reached a new plateau value (pH ≈ 3.52 to 3.72). Similar phenomenon was recurring during the photocatalytic oxidation of resorcinol at pH 2.8 in the presence of 5 mM Fe^{3+}. The pH of the solution increased and gradually levelled off ($pH_{final} \approx 3.9$). Furthermore, a control was also conducted in the absence of resorcinol and, again, the pH of solution was observed to increase from pH 3.3 to 3.6 when 1 mM Fe^{3+} was irradiated for 4 h in an aqueous suspension of TiO_2. Therefore, it is believed that the drop in activity at pH 2.8 in the presence of 5 mM Fe^{3+} and at pH 3.3 could be the result of short-circuiting reaction, in which the Fe^{2+}/Fe^{3+} couples create a cyclic process without the generation of ·OH. Alternatively, the reoxidation of Fe^{2+} could also take place in the presence of O_2 and HO_2· of which the later was formed from the reduction of molecular O_2 by a photogenerated electron. However, Catastini et al. [21] reported that the reoxidation of Fe^{2+} by O_2 occurred very slowly at acidic pH.

Fe^{3+} could have enhanced the oxidation rates via the photo-Fenton reaction, $Fe^{3+} + H_2O_2 + h\nu \rightarrow Fe^{2+} + {\cdot}OH + H^+$. Nonetheless, it has been argued that the production of H_2O_2 formed via the reduction of oxygen on illuminated TiO_2 is usually insignificant. Utset et al. [22] demonstrated that oxygen alone was incapable to induce the Fenton and photo-Fenton reactions. Furthermore, the production of H_2O_2 via photoexcitation of Fe^{2+} was also found to be difficult. Catastini et al. [21] also did not detect the presence of H_2O_2 when they irradiated Fe^{2+} in acid media. Hence, this highlights that the mechanism via photo-Fenton reaction may not be the main reaction by which the oxidation of resorcinol was enhanced.

The role of Fe^{3+} in enhancing the resorcinol oxidation could also be attributed to the involvement of homogeneous or surface complexes. However, the preliminary study revealed no complexation between resorcinol and Fe^{3+} in homogeneous solution for pH range of 1.5 to 3.3. The UV–vis spectra of resorcinol and Fe^{3+} mixtures were equal to the sum of the individual spectrum of resorcinol and Fe^{3+}. Despite this observation, further investigations are currently undertaken to identify the intermediate products of resorcinol and the possible formation of complex between the intermediate products of resorcinol and Fe^{3+}.

4. Conclusion

The performance of Fe^{3+} in the photocatalytic oxidation of resorcinol in the presence and absence of TiO_2 was investigated. Fe^{3+} enhanced the photochemical and photocatalytic oxidations of resorcinol at pH ⩽ 2 and the enhancement was attributed to the role of Fe^{3+} as an efficient source of ·OH. The Fe(III)-hydroxo complex photolysed efficiently under an irradiation of 360 nm yielding ·OH for the oxidation of resorcinol. $Fe(OH)^{2+}$ was believed to be the most photoactive species in the present system and its concentration in the solution was controlled by both pH and the total iron concentration. Furthermore, Fe^{3+} also played a role as an efficient electron scavenger in $UV/Fe^{3+}/TiO_2$ that suppressed the recombination of electron–hole pairs. At pH > 2, the presence of Fe^{3+} up to 1 mM improved the photochemical and photocatalytic oxidations of resorcinol, whereas at higher concentrations of Fe^{3+} (>1 mM), a retardation effect was observed. The formation of iron as $Fe(OH)_2{}^{4+}$, as well as the precipitation of iron as $Fe(OH)_3$ could have reduced the concentration of photoactive iron in the solution. In conclusion, it is clear that the kinetics of resorcinol oxidation is dependent on the nature of the Fe(III) species, both in the aqueous phase and adsorbed onto the photocatalyst.

References

[1] C. Groshart, P.C. Okkermann, Towards the Establishment of Priority List of Substances for Further Evaluation of Their Role in Endocrine Disruption, BKH Consulting Engineers, Delft, The Netherlands, 2000, p. 14.92.
[2] R.-A. Doong, R.A. Maithreepala, S.-M. Chang, Water Sci. Technol. 42 (2000) 253.
[3] H. Krysova, J. Jirkovsky, J. Krysa, G. Mailhot, M. Bolte, Appl. Catal. B 40 (2003) 1.
[4] S.W. Lam, K. Chiang, T.M. Lim, R. Amal, G.K.-C. Low, Appl. Catal. B 55 (2005) 123.
[5] N. Brand, M. Bolte, Chemosphere 40 (2000) 395.
[6] W. Feng, D. Nansheng, Chemosphere 41 (2000) 1137.
[7] R.W. Matthews, in: E. Pellizzetti, M. Schiavello, (Eds.), Photochemical Conversion and Storage of Solar Energy, Kluwer Academic, Netherlands, p. 427.
[8] J. Mack, J.R. Bolton, J. Photochem. Photobiol. A 128 (1999) 1.
[9] L. Lopes, J. de Laat, B. Legude, Inorg. Chem. 41 (2002) 2505.
[10] H. Mest'akova, G. Mailhot, J. Jirkovsky, J. Krysa, M. Bolte, Appl. Catal. B 57 (2005) 257.
[11] C.H. Langford, J.H. Carey, Can. J. Chem. 53 (1975) 2430.
[12] B.C. Faust, J. Hoigne, Atmos. Environ. 24A (1990) 79.
[13] R. Franck, W. Klopffer, Chemosphere 17 (1988) 985.
[14] H.-J. Benkelberg, P. Warneck, J. Phys. Chem. 99 (1995) 5214.
[15] M. Charles, J. Flynn, Chem. Rev. 84 (1984) 31.
[16] N. Brand, G. Mailhot, M. Bolte, J. Environ. Sci. Technol. 32 (1998) 2715.
[17] M. Mrowetz, E. Selli, J. Photochem. Photobiol. A 162 (2004) 89.
[18] P. Mazellier, M. Bolte, Chemosphere 42 (2001) 361.
[19] M.T. Emett, C.H. Khoe, Water Res. 35 (2001) 649.
[20] H. Mest'akova, G. Mailhot, J. Jirkovsky, J. Krysa, M. Bolte, Appl. Catal. B 58 (2005) 185.
[21] B. Utset, J. Garcia, J. Casado, X. Domenech, J. Peral, Chemosphere 41 (2000) 1187.
[22] C. Catastini, M. Sarakha, G. Mailhot, M. Bolte, Sci. Total Environ. 298 (2002) 219.